ESD-TR-76-308

Project Report

ETS-3

A. S. Friedman

Determination of Specular Reflection from Cylindrical Satellites for Electro-optical Surveillance and SOI

8 October 1976

Prepared for the Department of the Air Force
under Electronic Systems Division Contract F19628-76-C-0002 by

Lincoln Laboratory
MASSACHUSETTS INSTITUTE OF TECHNOLOGY
LEXINGTON, MASSACHUSETTS

The work reported in this document was performed at Lincoln Laboratory, a center for research operated by Massachusetts Institute of Technology, with the support of the Department of the Air Force under Contract F19628-76-C-0002.

This technical report has been reviewed and is approved for publication.

FOR THE COMMANDER

Raymond L. Loiselle, Lt. Col., USAF
Chief, ESD Lincoln Laboratory Project Office

MASSACHUSETTS INSTITUTE OF TECHNOLOGY

LINCOLN LABORATORY

DETERMINATION OF SPECULAR REFLECTION FROM CYLINDRICAL SATELLITES FOR ELECTRO-OPTICAL SURVEILLANCE AND SOI

A. S. FRIEDMAN

Group 94

PROJECT REPORT ETS-3

8 OCTOBER 1976

LEXINGTON MASSACHUSETTS

ABSTRACT

Although electro-optical satellite surveillance depends primarily upon diffuse solar reflection, an understanding of specular reflection can lead to enhanced detection and identification capability.

An analysis of the timing and duration of observable specular reflections has been completed for the widely applicable case of the cylindrical satellite. A solution is presented for geosynchronous satellites which includes orbital elements and attitude as parameters. This solution, in turn, is broadened to encompass misalignment of spin axis and symmetry axis.

A realization of the above computation in readily accessible, command-structured format has been developed as a planning aid for the GEODSS Experimental Test System. Samples of its output are provided, which record the occurrence of observable specular reflections in a convenient, easily understood calendrical tabulation.

Predicting the timing and duration of observable specular reflections is of considerable interest in the conduct of electro-optical satellite surveillance. Since a satellite may appear many magnitudes brighter when seen by specularly reflected sunlight than when seen only by diffusely reflected sunlight, this interest is quite understandable. Before providing an explanation of this phenomenon, let us turn to an example.

Figure 1 depicts a strip chart segment containing the optical signature (or light curve) of satellite 83525, as observed on 6 May 1976. The horizontal coordinate represents time, here amounting to a span of 90 s, and the vertical coordinate is proportional to satellite brightness. One function of a GEODSS site is the collection of strip charts such as this for further SOI analysis. An examination of the full strip chart reveals that the satellite is performing some sort of periodic gyration, as evidenced by the light curve's period of 40 s.

In order to assign consistent numerical values to brightness measurements, calibration readings of selected stars of known color and brightness must also be taken. [Figure 3]. This procedure provides values for night sky brightness and atmospheric extinction as well.

Figure 2 shows the light curve of the same satellite, this observation made on 25 March 1976. Comparison with Figure 1 reveals an increase in peak brightness of two magnitudes, which can be attributed to specular reflections. In this example the observations are separated by 42 days, but such an effect could arise in the space of 42 hours or 42 minutes.

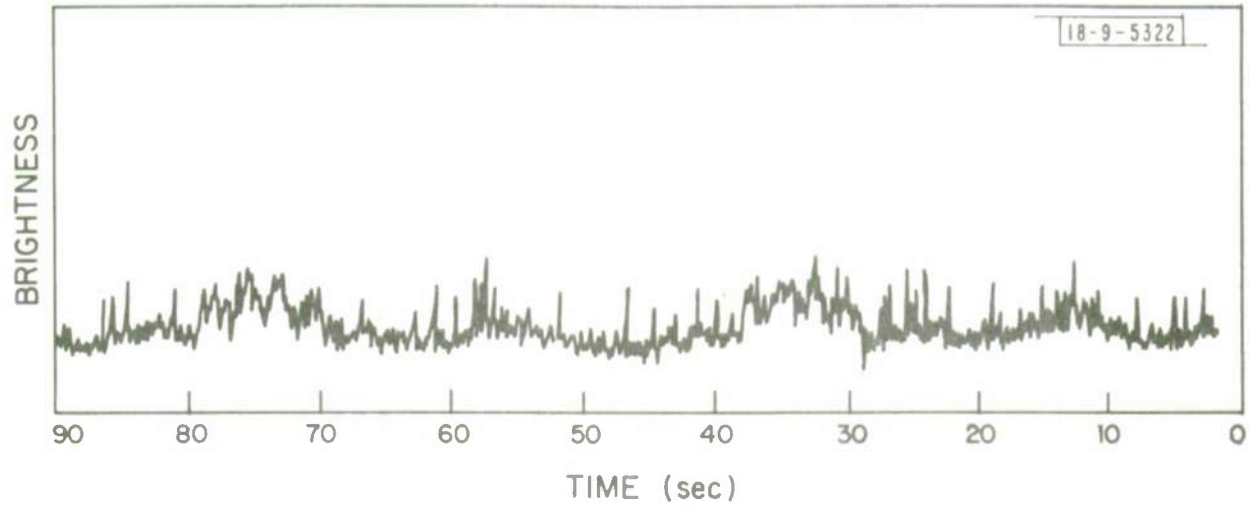

Fig. 1. Light curve of satellite, 83525 6 May 1976

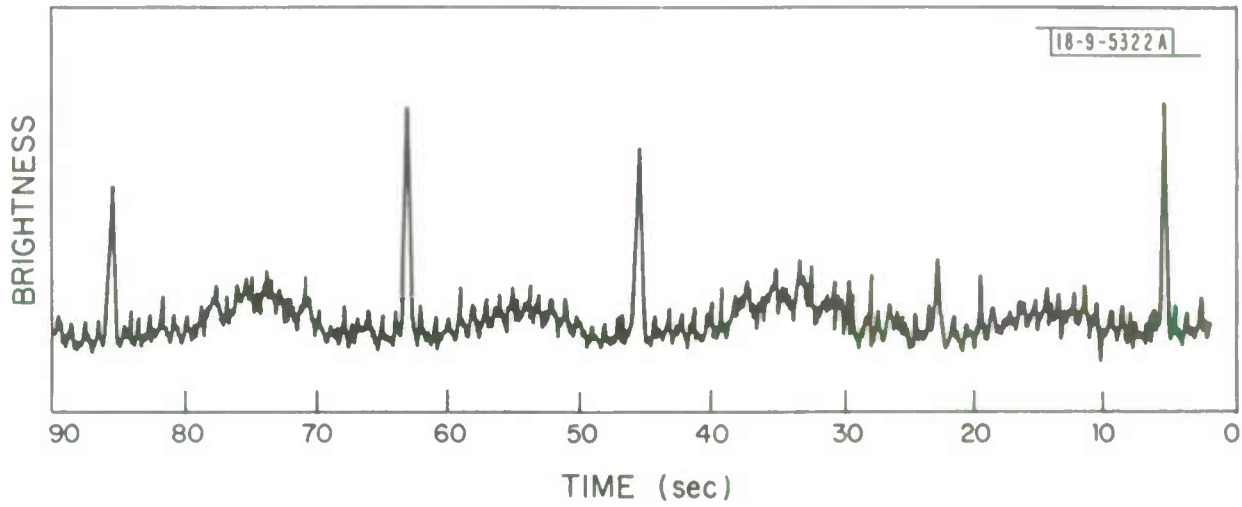

Fig. 2. Light curve of satellite, 83525 25 March 1976

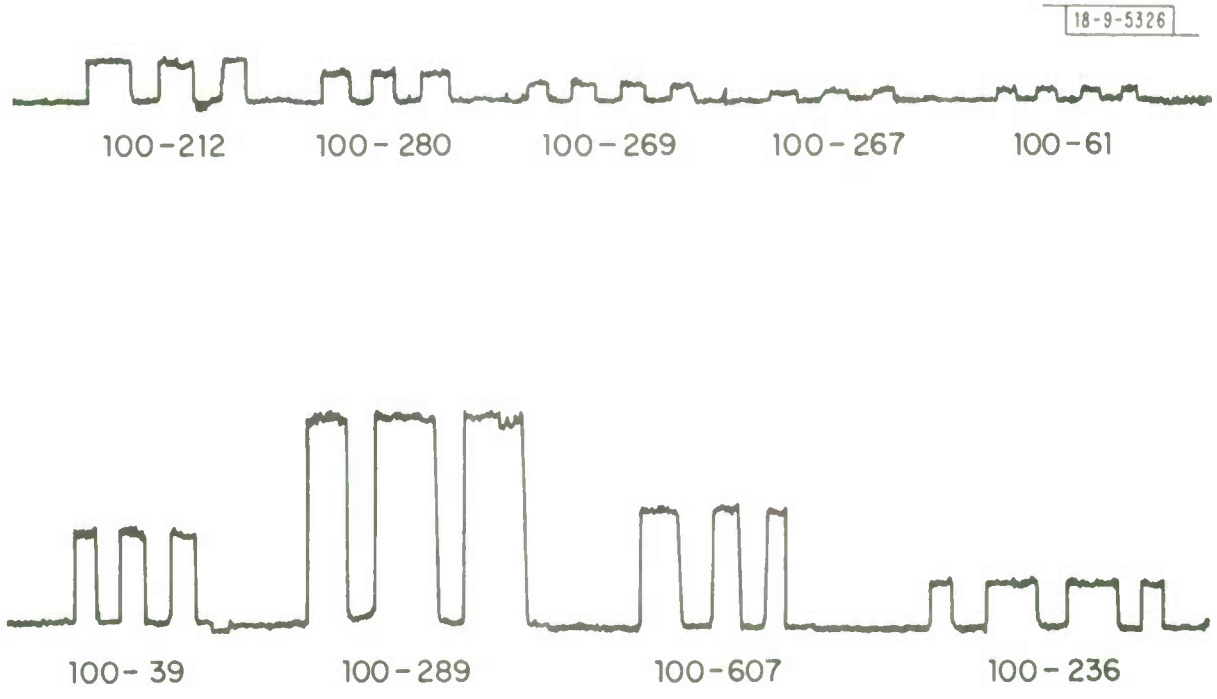

Fig. 3. Light curves, selected Landolt calibration stars

The mission of GEODSS does not include an SOI analysis of the fine structure of light curves, which is the domain of several other Air Force sponsored programs. But a preliminary examination of the light curve for such information as period and average brightness can vitally assist the surveillance role of GEODSS, by confirming the acquisition of a familiar satellite or by providing a means of distinguishing between satellites in the same vicinity. For this reason it is important to understand any phenomenon resulting in an anomalous change in brightness. Furthermore, a mastery of the timing of specular reflections can be a valuable scheduling asset, since maximum brightness should permit minimum search time. An extreme illustration is the case of satellite IMP-6, which was detected electro-optically on 24 October 1973 at a distance of 170,000 km - four times geosynchronous altitude - through the 31-inch telescope at Lowell Observatory. Had specular flashes not been visible, the satellite could not have been seen at all.

After so many repetitions of the term specular reflection, an explanation is now in order. Mirrorlike reflection from a shiny surface is termed specular, as distinguished from so-called diffuse reflection from an unpolished surface. Diffuse reflection is omnidirectional, while specular is limited in extent and consequently more concentrated. A single object may produce reflections of both types. With respect to satellites, it is diffusely reflected sunlight which ordinarily permits optical detection. Specular reflections, even if they occur, will be visible at a particular terrestrial location only when applicable geometric conditions are satisfied.

For a flat plate, the rule describing specular reflection is well-known: the angle of incidence equals the angle of reflection. This law is depicted in vectorial form in Figure 4. It may be readily extended to curved surfaces by measuring all angles from the normal at the point of reflection.

The chart in Figure 5 describes the current deployment of geosynchronous satellites launched before 1 January 1976. Observe that the large majority have cylindrical bodies. Such satellites are usually faced with solar cells, which are known to be specular reflectors, and for these a specularly reflecting cylinder serves as a good mathematical model. We will limit our attention to this important category, diagrammed in Figure 6. Light rays incident upon the cylinder from a single direction diverge, after reflection, in a multidirectional configuration whose shape is approximately conical. As seen from a sufficiently great distance, that configuration can be regarded as a perfect right circular cone, coaxial with the cylinder and making the same angle with its axis as does the incoming light. [Figure 7].

In the case of solar illumination, the sun may be considered a remote disk of angular diameter one-half degree. Its reflected light thus constitutes a "thickened" cone, of angular thickness one-half degree, as illustrated in Figure 8. Let us now inquire how these reflections impinge upon the earth.

As a preliminary simplification, Figure 9 depicts a spherical earth and an ideal geosynchronous satellite, cylinder axis parallel to the

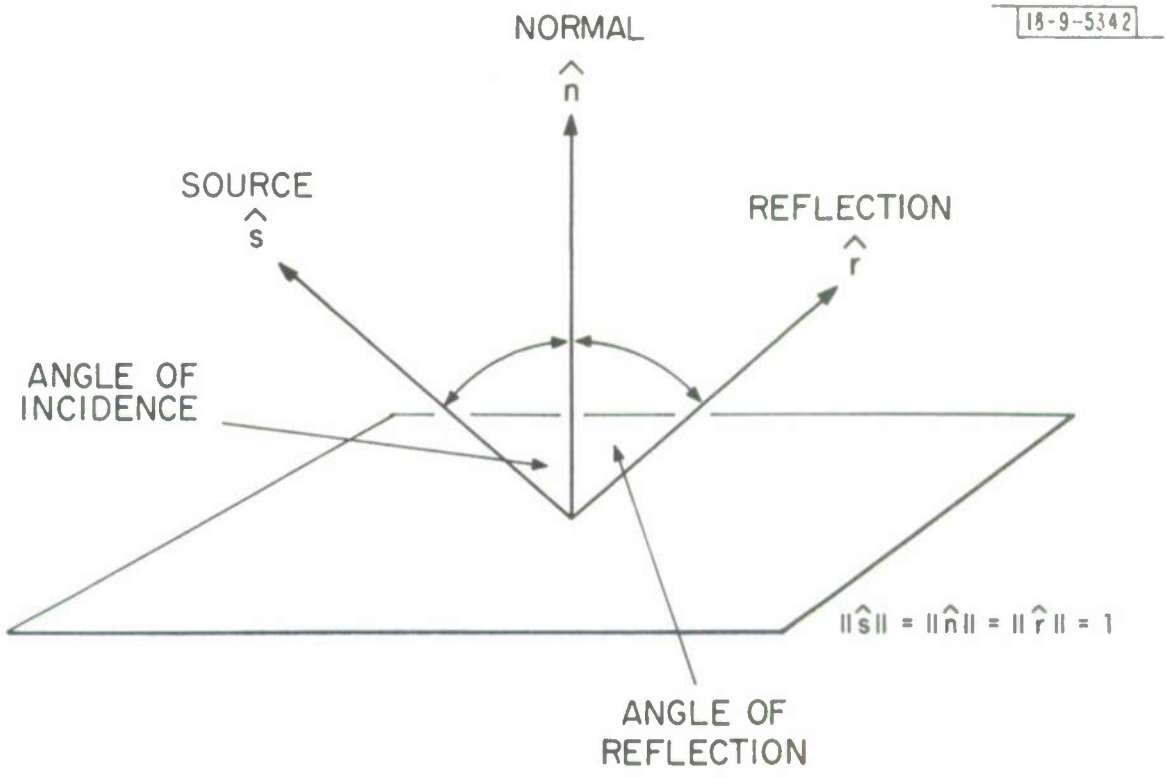

$$\hat{r} = -\hat{s} + 2(\hat{s} \cdot \hat{n})\hat{n}$$

Fig. 4. Specular reflection from a flat plate-vector representation

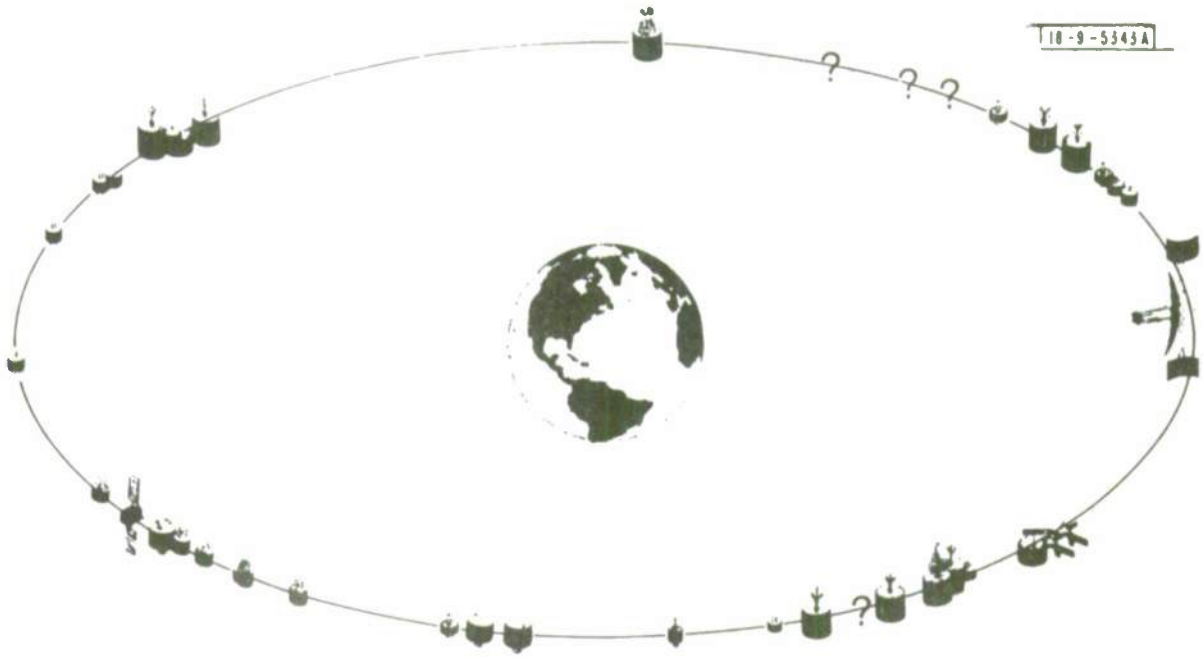

Fig. 5. Geosynchronous satellites launched before 1 January 1976 [Adapted from Comsat Technical Review, vol. 6, no. 1, pp. 196-197]

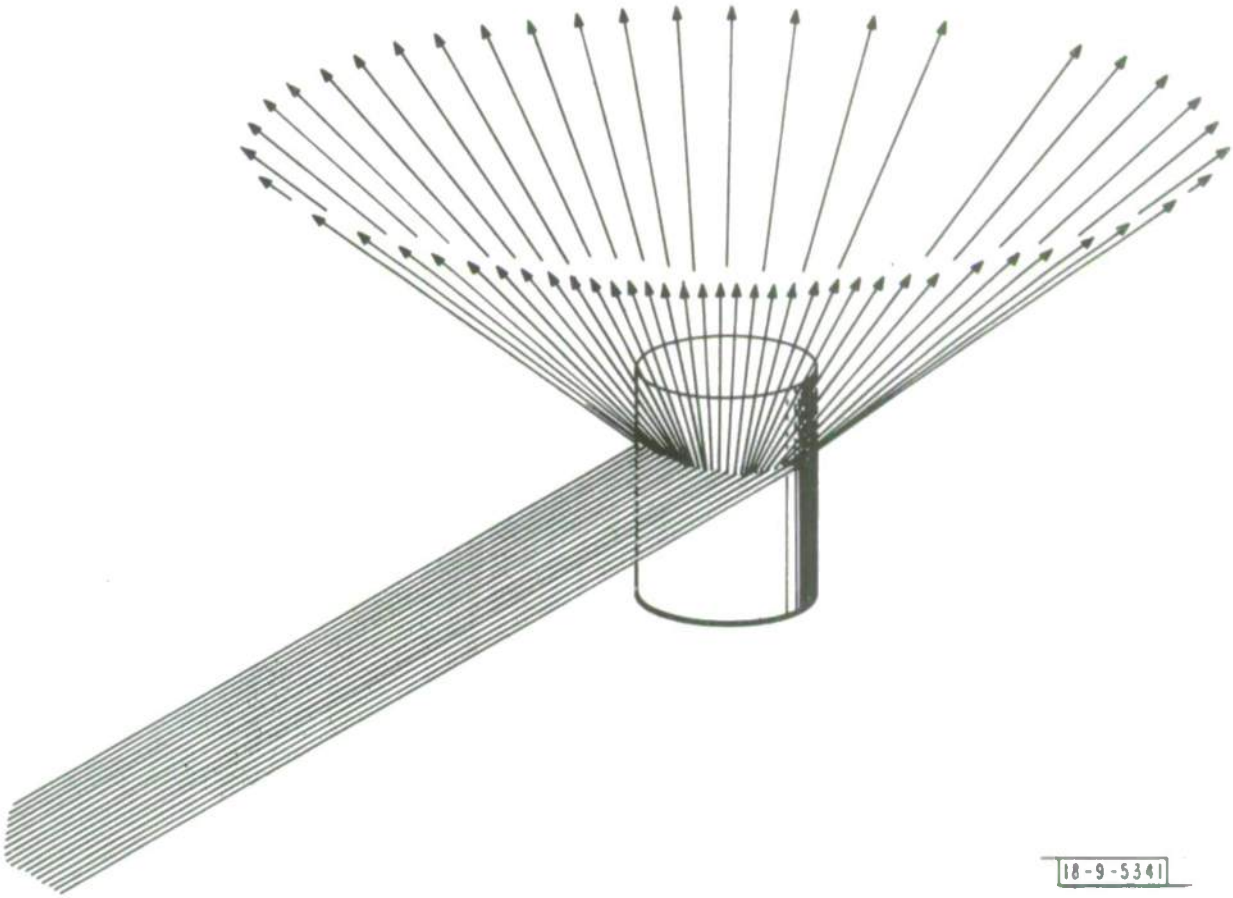

Fig. 6. Specular reflection from a cylinder (close up view)

Fig. 7. Specular reflection from a cylinder

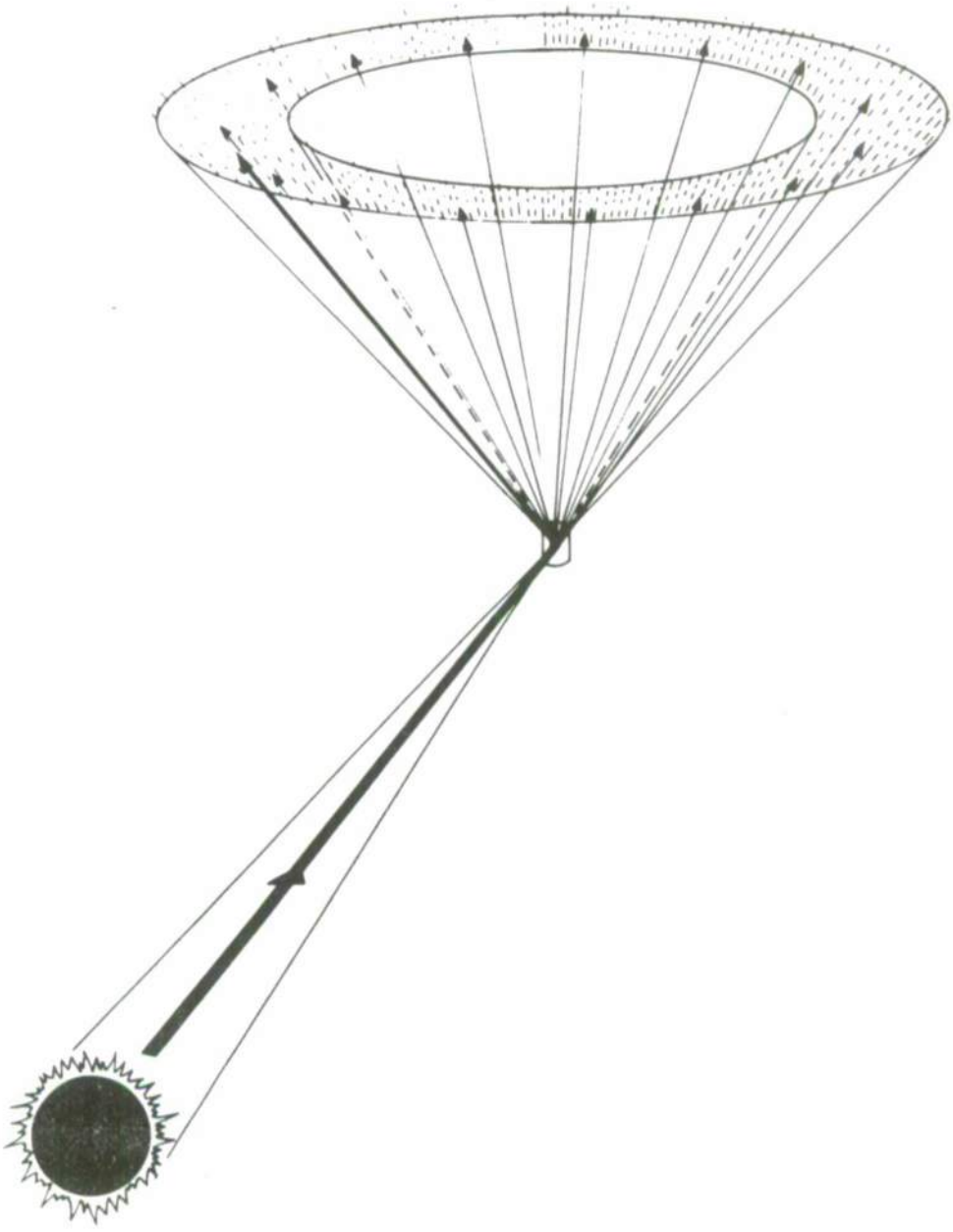

Fig. 8. Solar specular reflection from a cylinder (not to scale)

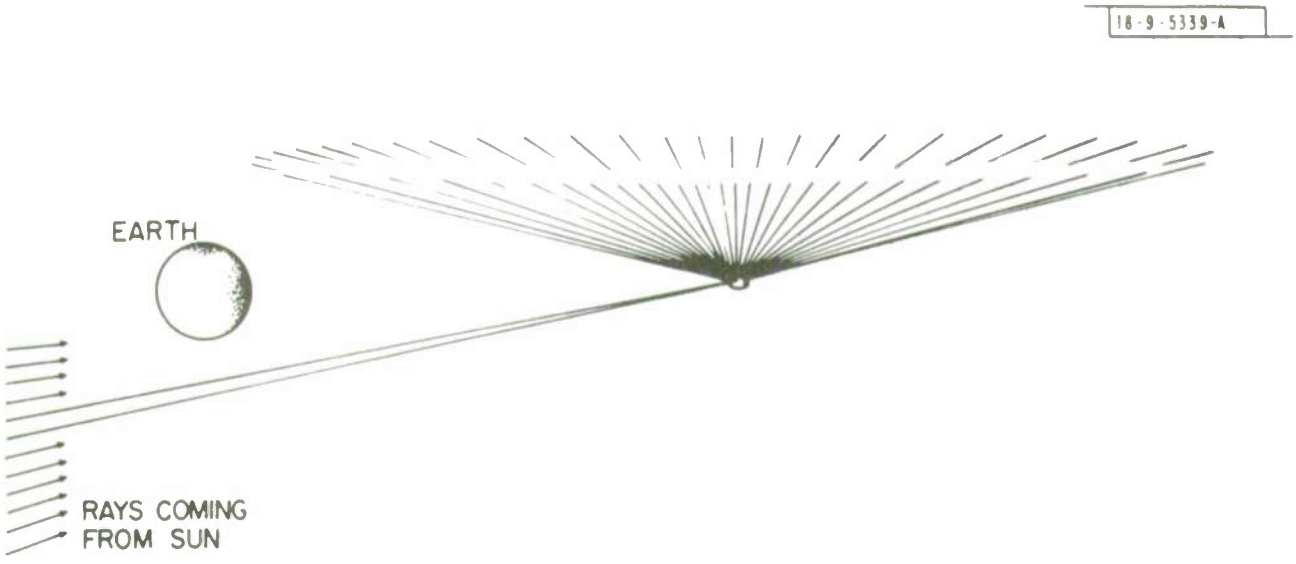

Fig. 9. Terrestrial visibility of solar specular reflection (unfavorable solar declination

earth's. The sun's declination is such that no specularly reflected rays reach the terrestrial observer. In Figure 10, however, the opposite case is shown, only the rays striking the earth being included. According to the indicated trigonometric relationships, specular reflections are observable at a site of latitude ϕ and sub-satellite longitude if and only if the declination of the source, δ, satisfies the following equation:

$$\tan \delta = \frac{\sin \phi}{\cos \phi - (R_s/R_e)} \quad , \qquad \text{(A)}$$

where $R_s \approx 42,164$ km is geosynchronous distance, $R_e \approx 6,378$ km is the earth's radius, and hence $(R_s/R_e) \approx 6.61$. Since the source may be any location on the sun's disk, equation (A) is equivalent to the following constraint on solar declination, $\delta_\odot$:

$$\left| \delta_\odot - \arctan \left(\frac{\sin \phi}{\cos \phi - 6.61} \right) \right| \leq 0.5^\circ. \qquad \text{(B)}$$

Hence, specular reflections are observable at just those times when $\delta_\odot$ assumes values in a specific interval, functionally related to site latitude.

The cyclic variation of solar declination is an aspect of the annual course of the seasons, as shown in Figure 11. As a result, each value of solar declination corresponds to two dates. When ϕ is restricted to northern temperate latitudes, for example, the limitations on $\delta_\odot$ imposed by equation (B) are seen to confine specular observability

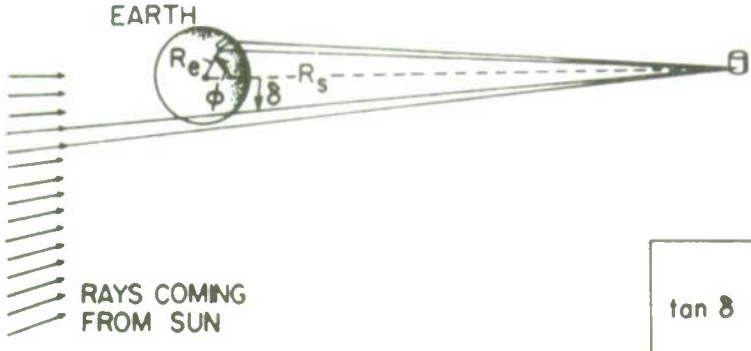

$$\tan \delta = \frac{\sin \phi}{\cos \phi - (R_s / R_e)}$$

Fig. 10. Terrestrial visibility of solar specular reflection (favorable solar declination)

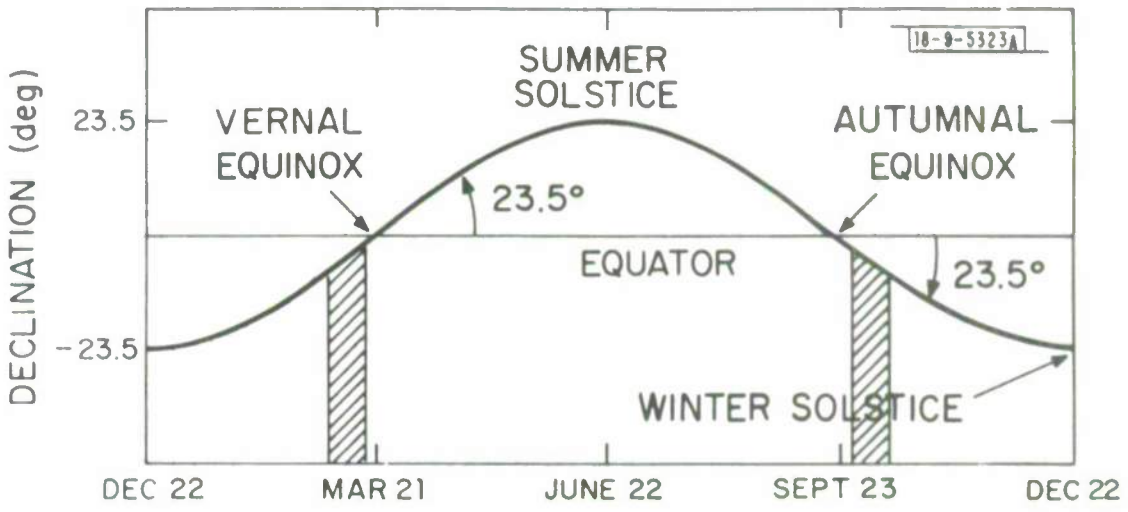

Fig. 11. Annual cycle of solar declination

to one period shortly before the vernal equinox and another shortly after the autumnal, each lasting less than two weeks. The mean rate of change of $\delta_\odot$ then being about $.38^\circ$/day, the duration of specular observability at any individual site will be approximately 32 hours, part of which will occur during daylight.

Although in the real world the above simplifying assumptions do not hold, the following valid conclusion can be drawn: at a north temperate zone site (such as the Lincoln Laboratory GEODSS Test Site), specular reflections will be prevalent around the time of the equinoxes, particularly before the vernal and after the autumnal. As a corollary, if system detection capability is to be tested under least favorable brightness conditions, sensitivity measurements should be taken near the summer solstice.

A more accurate model of specular timing must take account of all deviations of the satellite orbital elements from true geosynchronous. Likewise, variations in spin axis orientation (also called attitude) must be considered. Satellites which are not perfectly balanced may in addition seem to wobble, as shown in Figure 12. This motion represents a misalignment of the cylinder's spin axis and symmetry axis, which can significantly lengthen the specular viewing period.

The above computational requirements can best be satisfied by a computer program. If it is to serve as a practical planning tool, it must be readily accessible at each GEODSS site, and its results must be provided in a convenient format. The author has written such a program

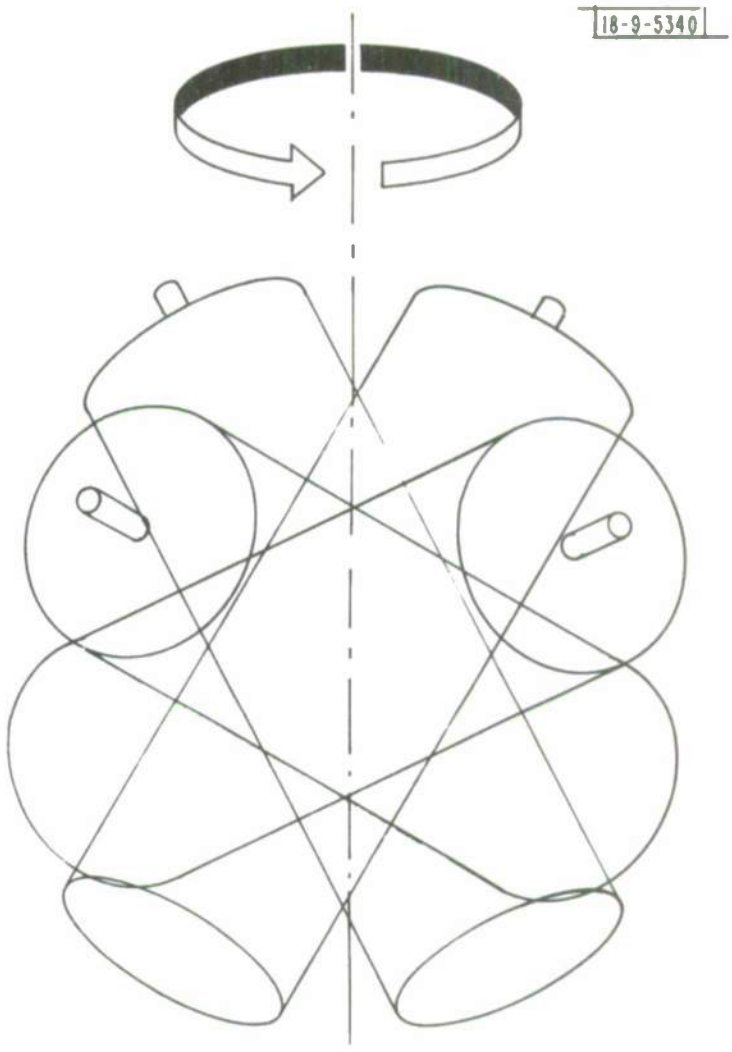

Fig. 12. Wobbling cylinder (spin axis and symmetry axis misaligned)

for the MODCOMP IV minicomputer, an example of whose output is shown in Figure 13. It takes the form of a graphic table, each row representing an observing night, each column an observing time, at ten minute intervals. In addition to observable specular reflections, indicated by (*), the chart specifies the following phenomena: sunset/sunrise (S), twilight (T), eclipse by earth (E), and (for satellites with strong sublongitude drift) descent below horizon (X). The program is interactive and command structured. The computation of a month's specular reflections takes under a minute.

The chart in Figure 13 refers to the true geosynchronous case described above, as seen from a site of latitude 35° and longitude 0°. Figures 14-16 illustrate timing changes resulting from the alteration of a single parameter. The respective modifications are: site moved to latitude 25°; orbital inclination of 0.5° introduced; axial offset of 0.2° introduced.

When the orbital elements or other parameters are not known exactly, the specular predictions will also contain uncertainty. For example, a change of 0.1° in inclination may cause a shift of as much as six hours in specular observability, and a like change in attitude may have a 12 hour response. When the objective is to recognize a satellite by its known diffuse return, a reasonable precaution is to augment the predicted specular period by a buffer period incorporating recognized uncertainty. When the objective is to capitalize on specular brightness for detection, one should schedule observations near the center of the longest specular

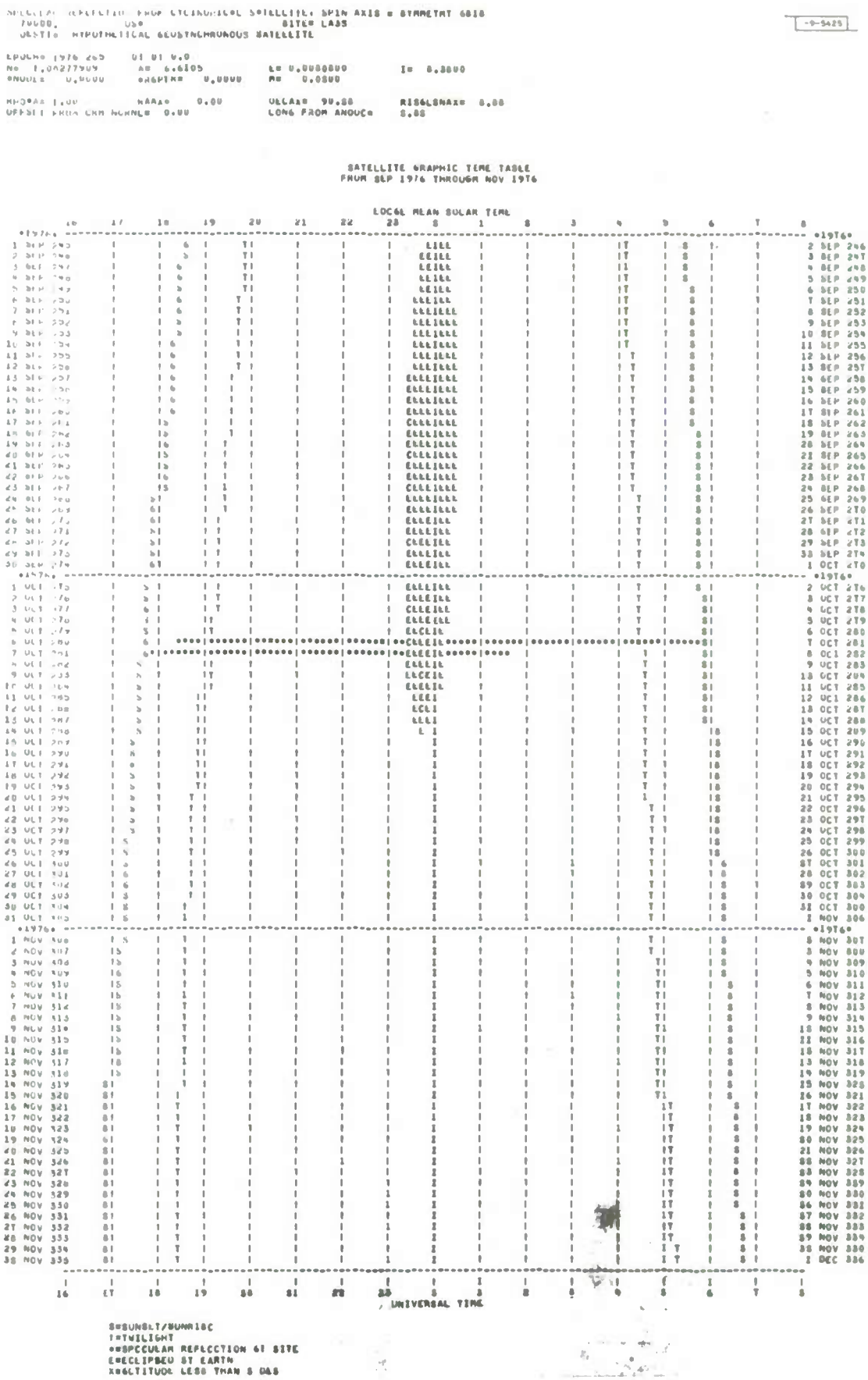

Fig. 13. Specular reflection visibility chart

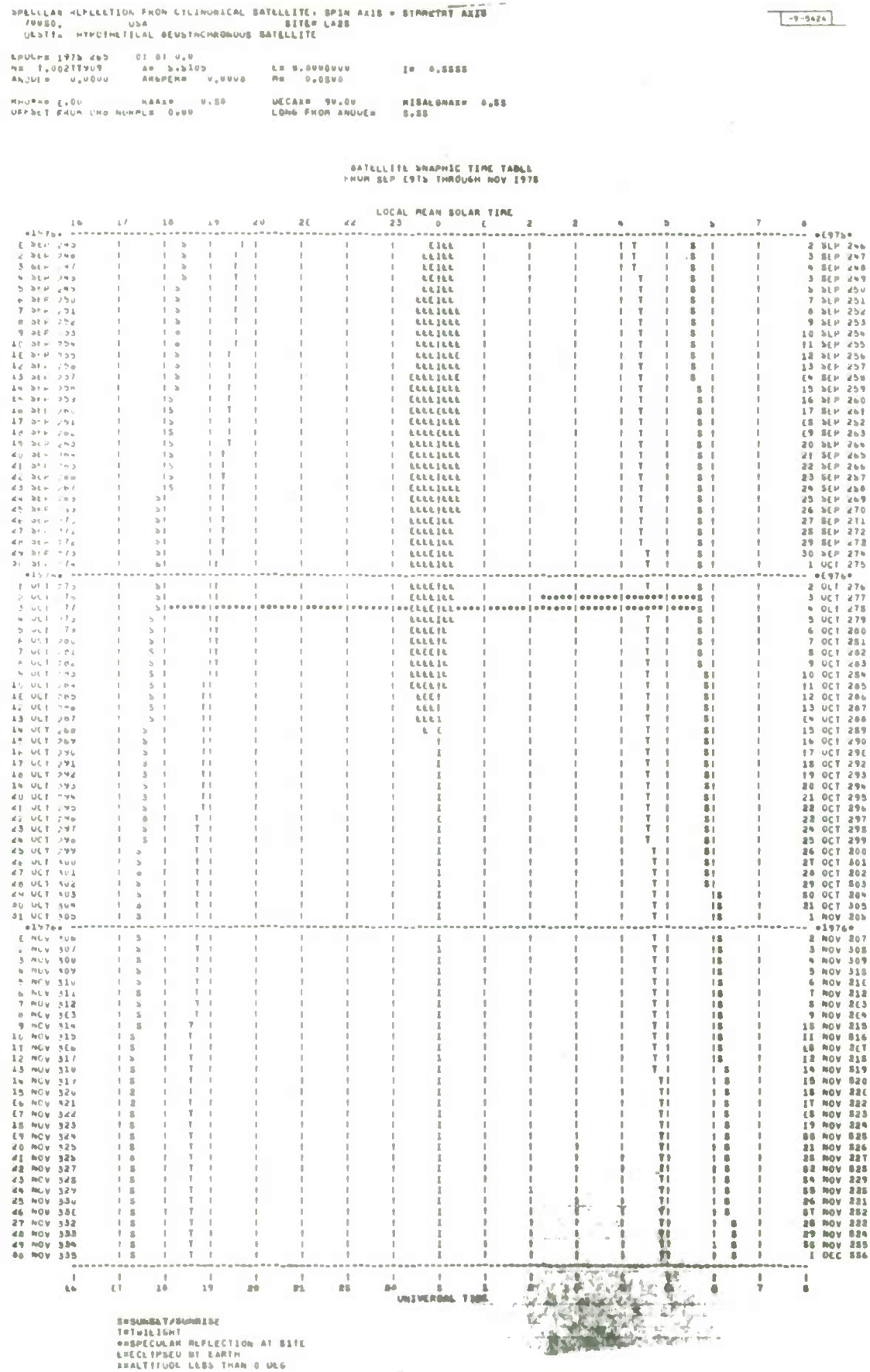

Fig. 14. Specular reflection visibility chart (change in site latitude of 10^{o})

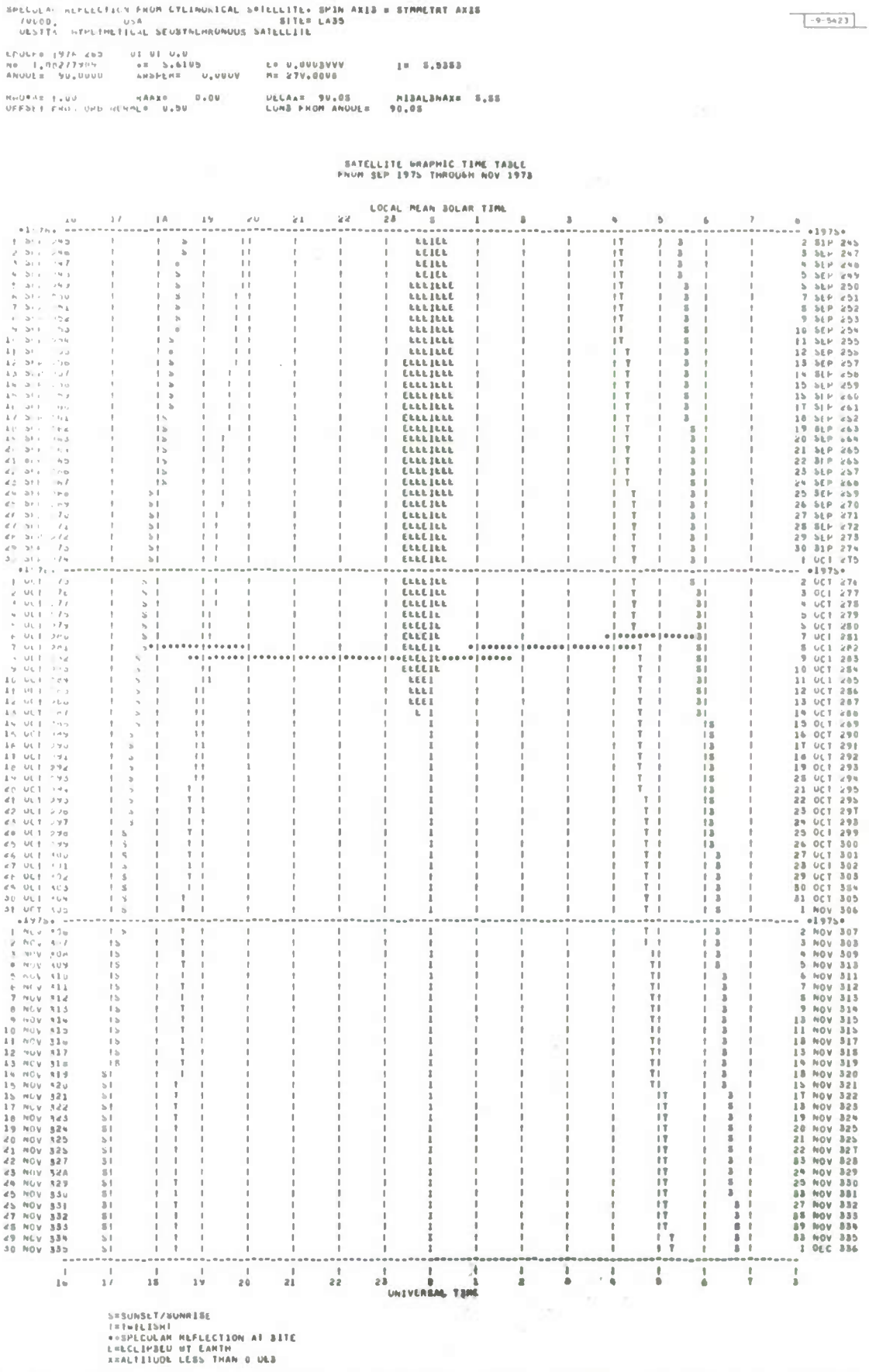

Fig. 15. Specular reflection visibility chart (change in orbital inclination of 0.5^{o})

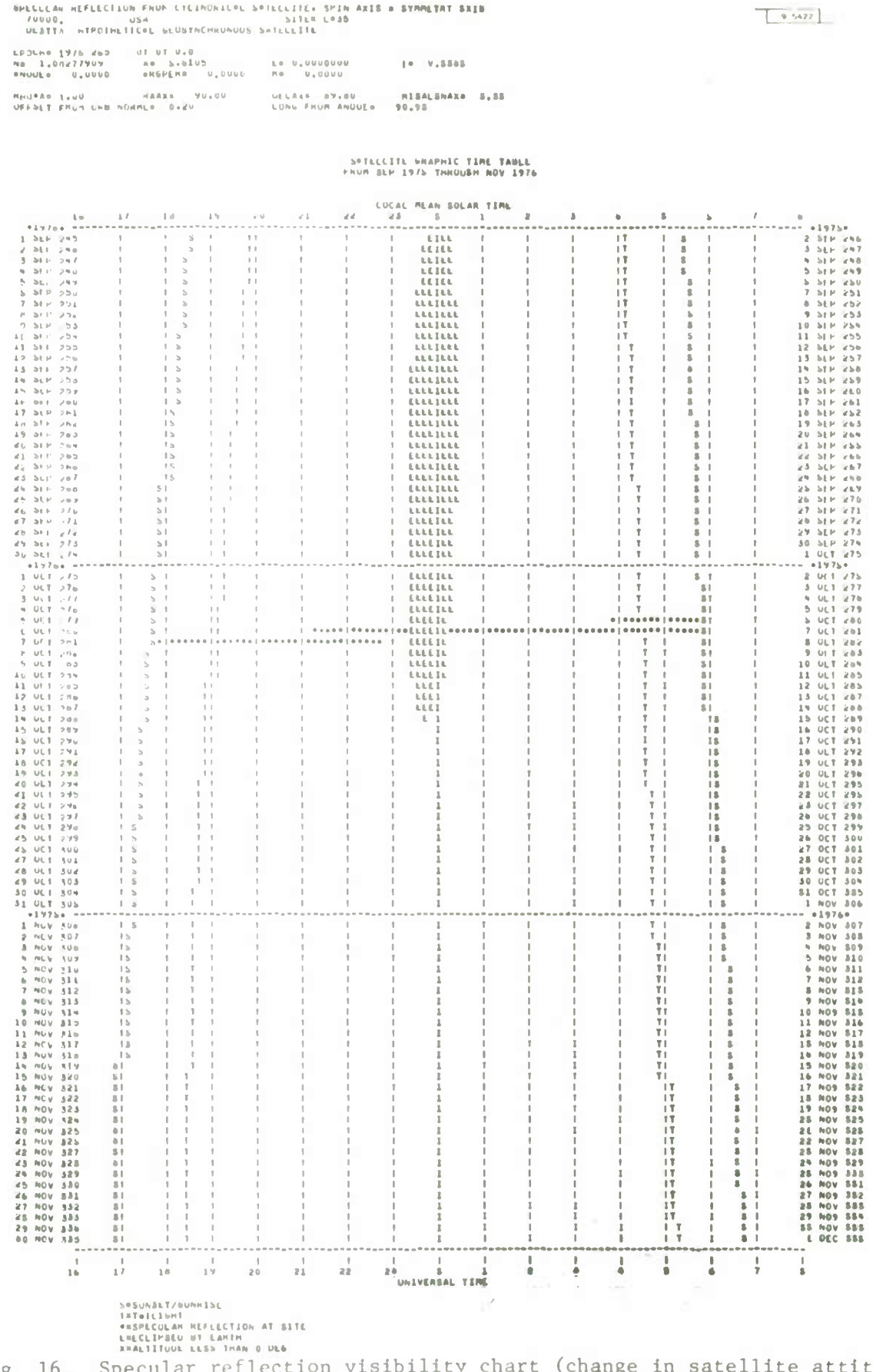

Fig. 16. Specular reflection visibility chart (change in satellite attitude of 0.2^{o})

periods available. In either case, the program facilitates tentative parameter modification, so that alternate predictions may be obtained for comparison.

The case of the wobbling satellite deserves further comment. As the satellite spins about a fixed axis, its symmetry axis revolves about that spin axis because of their misalignment. As a result, the geometric requirements for specular reflection may be satisfied during some portions of a spin period and unsatisfied during others. The relevant concept is the envelope of all specular rays which may periodically be reflected. This envelope is closely related to the classical limaçon of Pascal (cf. Figure 17) and can be described by a closed parametric formula. The shape of the resulting envelope is approximated in Figure 18. It still resembles a thickened cone, but the thickening is uneven and depends upon the amount of misalignment. Figure 19 shows our standard example with an introduced misalignment of 0.5°. Figure 20 shows a less artificial example, with orbital inclination of 5.7°, offset of 2.8°, and misalignment of 0.5°.

Extensive observations based on the above analysis are planned for the 1976 autumnal equinox. Already at hand are data from February and March, 1976, concerning Lincoln Experimental Satellite 6. LES-6 is particularly interesting because of its large misalignment of 2.2° and its unfavorable altitude at the Lincoln GEODSS site of less than 12° above the horizon. Pronounced specular returns were obtained at the times indicated in Figure 21, which are quite compatible with predicted

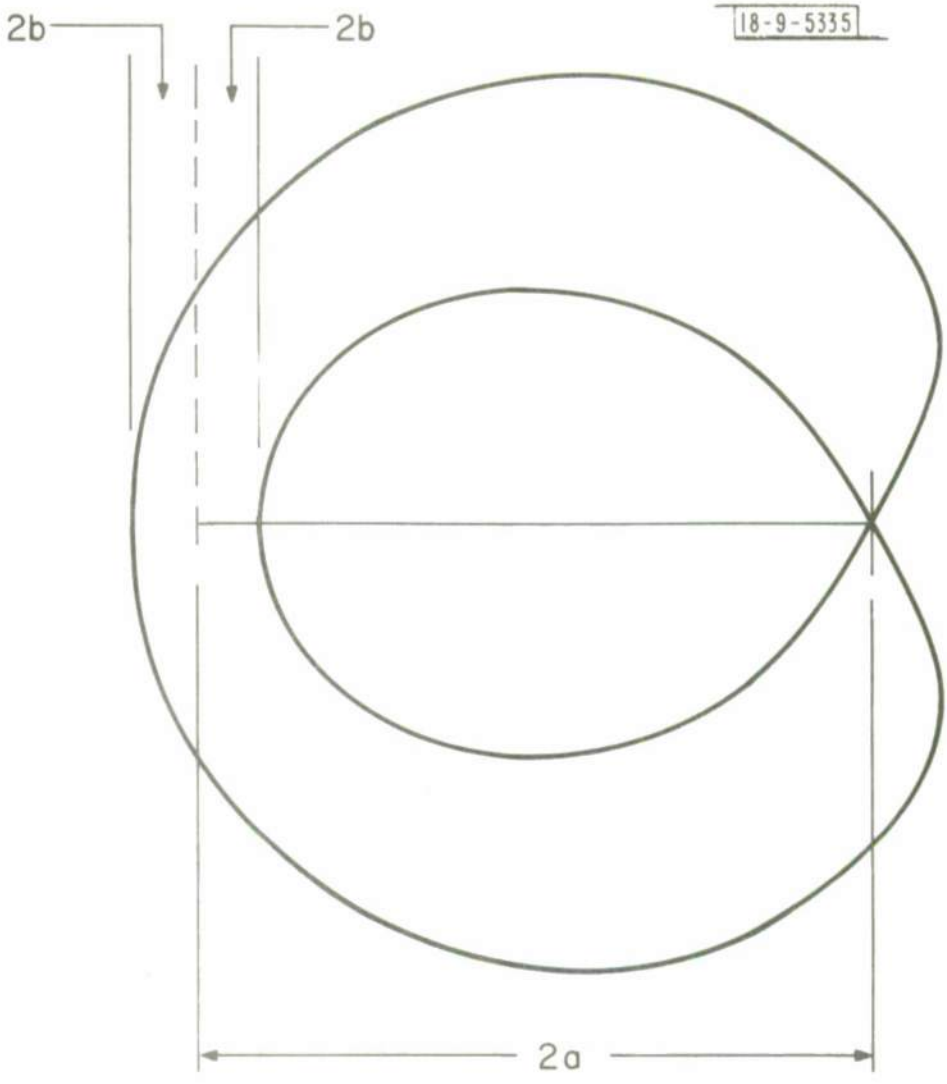

$$r = 2(b - a\cos\theta)$$

$$(x^2 + y^2 + 2ax)^2 = 4b^2(x^2 + y^2)$$

Fig. 17. Limaçon of Pascal

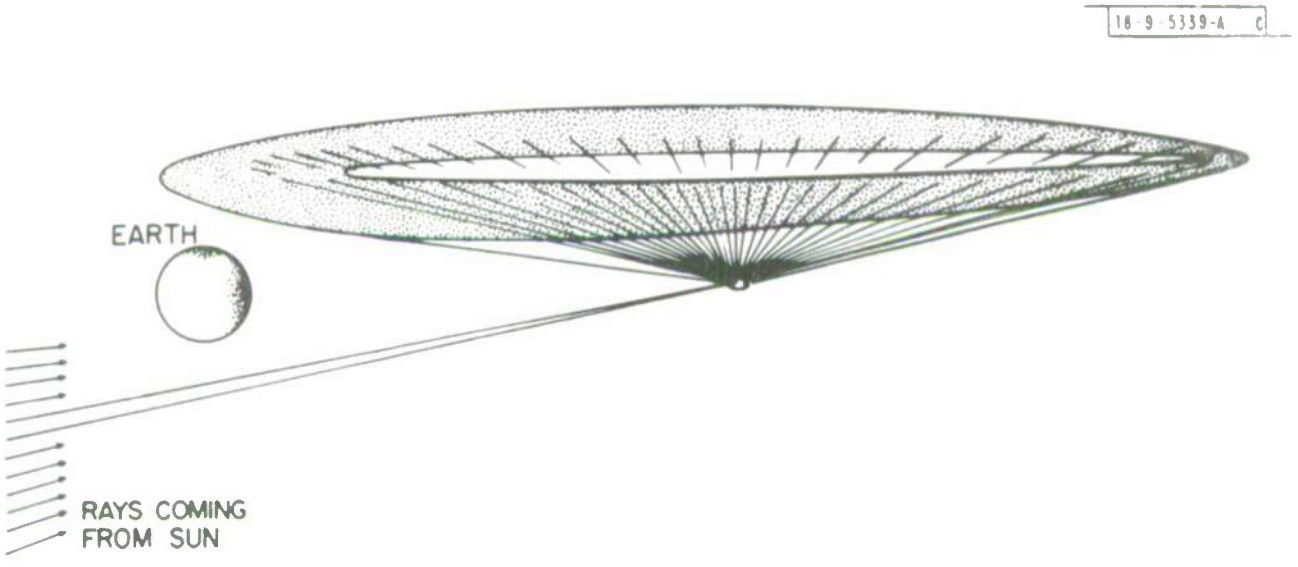

Fig. 18. Terrestrial visibility of solar specular reflection (wobbling satellite)

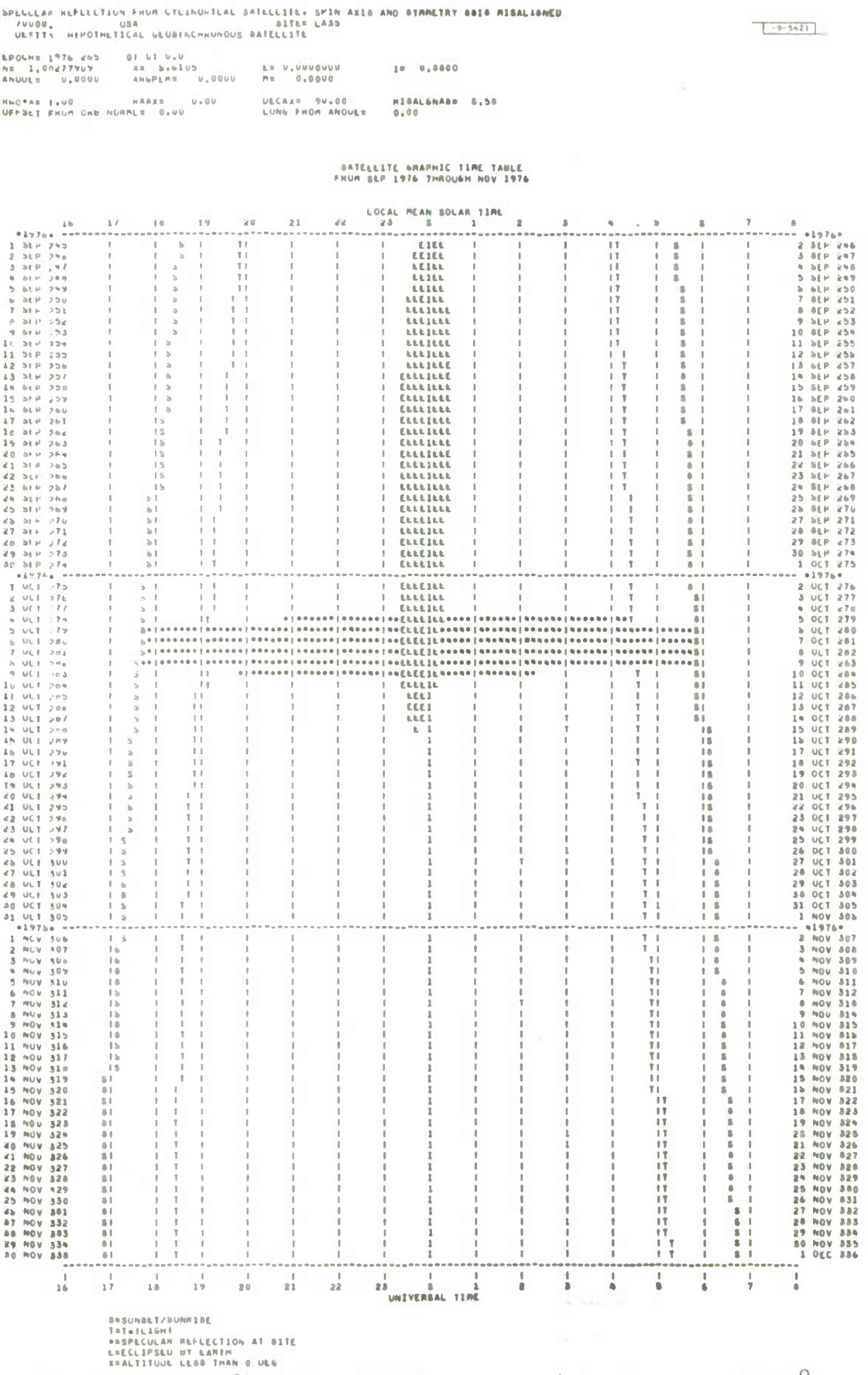

Fig. 19. Specular reflection visibility chart (misalignment of 0.5° introduced)

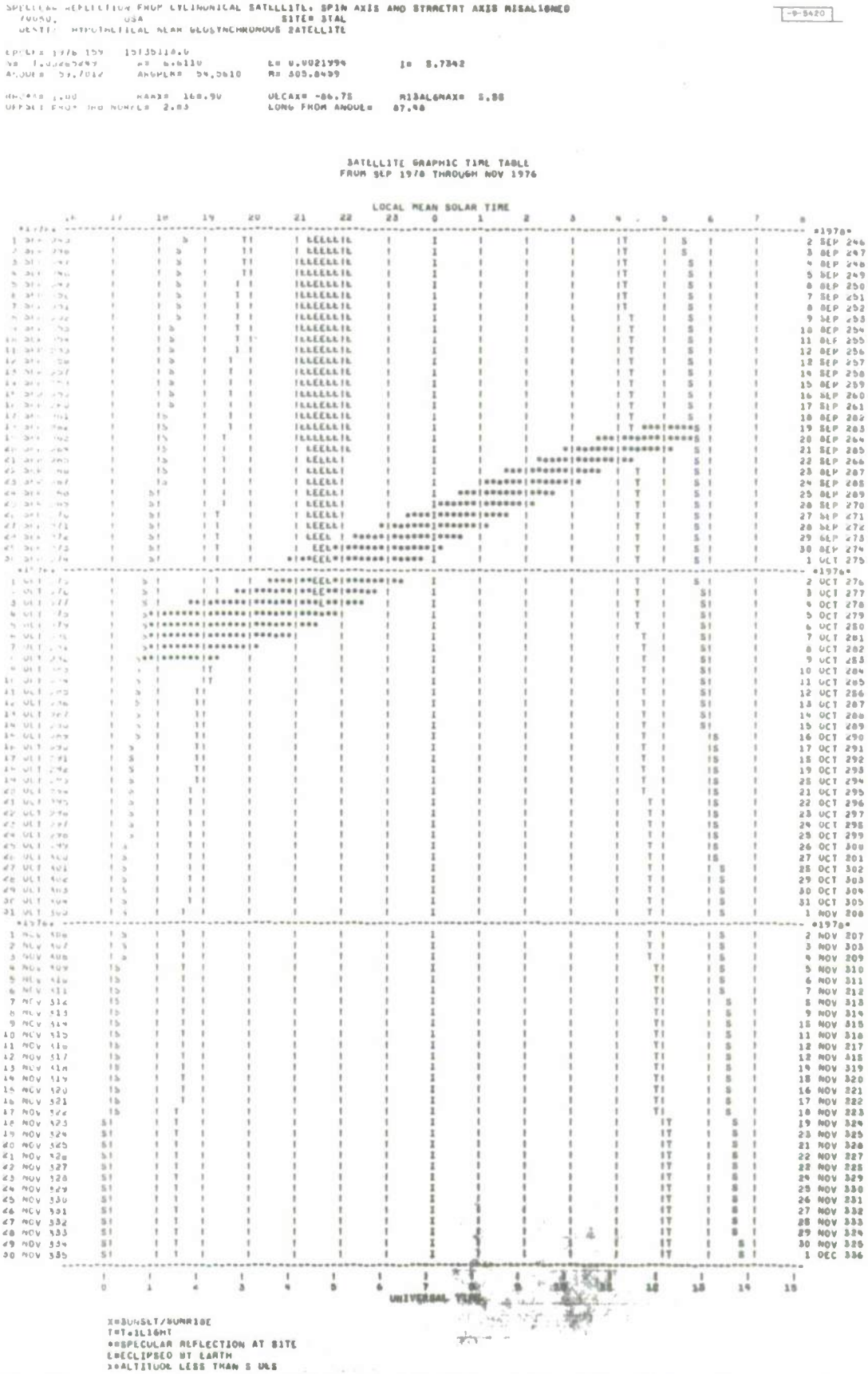

Fig. 20. Specular reflection visibility chart (misalignment present)

Fig. 21. Specular reflection visibility chart (LES-6 - Spring, 1976)

timing. A record of unsuccessful observation attempts for similar comparison would have been most desirable and will be included in the fall observing program.

UNCLASSIFIED

SECURITY CLASSIFICATION OF THIS PAGE *(When Data Entered)*

REPORT DOCUMENTATION PAGE		READ INSTRUCTIONS BEFORE COMPLETING FORM
1. REPORT NUMBER ESD-TR-76-308	2. GOVT ACCESSION NO.	3. RECIPIENT'S CATALOG NUMBER
4. TITLE *(and Subtitle)* Determination of Specular Reflection from Cylindrical Satellites for Electro-optical Surveillance and SOI		5. TYPE OF REPORT & PERIOD COVERED Project Report 6. PERFORMING ORG. REPORT NUMBER Project Report ETS-3
7. AUTHOR*(s)* Alan S. Friedman		8. CONTRACT OR GRANT NUMBER*(s)* F19628-76-C-0002
9. PERFORMING ORGANIZATION NAME AND ADDRESS Lincoln Laboratory, M. I. T. P. O. Box 73 Lexington, MA 02173		10. PROGRAM ELEMENT, PROJECT, TASK AREA & WORK UNIT NUMBERS Program Element No. 63428F Project No. 2128
11. CONTROLLING OFFICE NAME AND ADDRESS Air Force Systems Command, USAF Andrews AFB Washington, DC 20331		12. REPORT DATE 8 October 1976 13. NUMBER OF PAGES 34
14. MONITORING AGENCY NAME & ADDRESS *(if different from Controlling Office)* Electronic Systems Division Hanscom AFB Bedford, MA 01731		15. SECURITY CLASS. *(of this report)* Unclassified 15a. DECLASSIFICATION DOWNGRADING SCHEDULE

16. DISTRIBUTION STATEMENT *(of this Report)*

Approved for public release; distribution unlimited.

17. DISTRIBUTION STATEMENT *(of the abstract entered in Block 20, if different from Report)*

18. SUPPLEMENTARY NOTES

None

19. KEY WORDS *(Continue on reverse side if necessary and identify by block number)*

specular reflection
cylindrical satellites
electro-optical surveillance
space object identification (SOI)

20. ABSTRACT *(Continue on reverse side if necessary and identify by block number)*

An analysis of the timing and duration of observable specular reflections from cylindrical satellites is presented, taking into account orbital elements, attitude, and axial misalignment (wobble). Results are displayed in the form of computer-generated graphic tables.

DD FORM 1 JAN 73 1473 EDITION OF 1 NOV 65 IS OBSOLETE

UNCLASSIFIED

SECURITY CLASSIFICATION OF THIS PAGE *(When Data Entered)*